# Climate Change Projections for the Wooli Wooli Estuary and Batemans Bay

Ian Macadam, Kathleen McInnes and Julian O'Grady
4 September 2007

A report for the New South Wales Department of Environment and Climate Change

# CONTENTS

# EXECUTIVE SUMMARY

The NSW Department of Environment and Climate Change is undertaking a preliminary investigation into the impacts of climate change on estuaries along the New South Wales (NSW) coastline. Two study locations, the Wooli Wooli River system and the Clyde River/Batemans Bay system, have been selected. It is expected that the study of these two very different estuary systems will facilitate the assessment of the impacts of climate change on other estuaries on the NSW coast.

This report draws on existing literature to provide information on changes in climate variables likely to impact the Wooli Wooli Estuary and Batemans Bay for the 2030 and 2070 planning horizons. It complements a report by McInnes et al. (2007) describing projected changes in environmental variables that influence coastal erosion for the same two locations and planning horizons.

There are three main sources of uncertainty to be considered when producing projections of global warming-induced climate change for a region for a given year in the future:

1) The uncertainty in the future evolution of greenhouse gas concentrations in the atmosphere.

2) The uncertainty in how much the global average surface temperature will respond to increases in atmospheric greenhouse gas concentrations.

3) The uncertainty in how changes to the climate as a result of global warming will vary spatially and hence how the climate of the region under consideration will respond to an increase in global average surface temperature.

The first uncertainty can be addressed by considering the future evolution of atmospheric greenhouse gas concentrations arising from the Intergovernmental Panel on Climate Change's SRES emission scenarios (IPCC, 2000). The second uncertainty can be addressed by considering the future rates of future global warming in simulations of different climate models forced with increases in atmospheric greenhouse gas concentrations arising from the SRES emission scenarios. The third uncertainty can be addressed by considering the spatial patterns of climate change in multiple climate models.

Most of the climate change projections given in the McInnes et al. (2007) report that accompanies this report were based on the output of two climate model simulations, "CCM2" and "CCM3". In this report, where they have been available, projections derived from the same two simulations have been presented in order to describe climate change scenarios that are consistent with the information from the work of McInnes et al. (2007). These are summarised in Tables S1 and S2. Both simulations were forced with historical atmospheric greenhouse gas concentrations until 1990 and with estimates of future atmospheric greenhouse gas concentrations arising from the SRES A2 emission scenario from then on. The SRES A2 emission scenario, under which atmospheric carbon dioxide concentrations rise from their present level of about 370ppm to about 880ppm by 2100, yields approximately mid-range values of global warming. However, for some climate variables it has been possible to take the range of future rates of global warming arising from the complete set of SRES emission scenarios into account and, for each of 2030 and 2070, projections for a low-end global warming value and a high-end global warming value have been given for each of the CCM2 and CCM3 simulations. Hence, for these variables, projections for four plausible scenarios of regional climate change, "CCM2 Low GW", "CCM2 High GW", "CCM3 Low GW" and "CCM3 High GW", have been given.

In addition to the climate change projections presented in Tables S1 and S2, projections that include information from climate simulations other than CCM2 and CCM3 are available for rainfall extremes. These are summarised in Table S3.

***Table S1:*** *Summary of climate change projections for the Wooli Wooli Estuary for 2030 and 2070 derived from the CCM2 and CCM3 simulations. Changes in mean sea level are relative to global average mean sea level rise, which is projected to be 0.18 to 0.79m by 2095, relative to the global average mean sea level for 1990. Other changes are relative to climatological averages for 1990. Unsigned numbers in red indicate increases. Numbers in blue indicate decreases. Source: Holper et al. (2006) and McInnes et al. (2007).*

| 2030 | | | | 2070 | | | |
|---|---|---|---|---|---|---|---|
| CCM2 Low GW | CCM2 High GW | CCM3 Low GW | CCM3 High GW | CCM2 Low GW | CCM2 High GW | CCM3 Low GW | CCM3 High GW |
| **Changes in annual average daily maximum air temperatures (°C)** | | | | | | | |
| 0.5 | 1.2 | 0.6 | 1.3 | 1.1 | 3.6 | 1.2 | 4.0 |
| **Changes in annual average daily minimum air temperatures (°C)** | | | | | | | |
| 0.5 | 1.1 | 0.6 | 1.3 | 1.1 | 3.5 | 1.2 | 4.0 |
| **Changes in annual average rainfall totals (%)** | | | | | | | |
| -3 | -6 | 0 | 0 | -6 | -19 | 0 | -1 |
| **Changes in annual average solar radiation (%)** | | | | | | | |
| 0.3 | 0.6 | 0.2 | 0.5 | 0.6 | 1.8 | 0.5 | 1.6 |
| **CCM2** | | **CCM3** | | **CCM2** | | **CCM3** | |
| **Annual dominant wind direction** | | | | | | | |
| SE (112.5 to 157.5°) | | | | | | | |
| **Changes in the frequency of annual dominant wind direction days with average wind speeds greater than 8m/s (%)** | | | | | | | |
| -4 | | 5 | | -8 | | 9 | |
| **Changes in the 1-in-100 year storm surge height (%)** | | | | | | | |
| -1 | | 1 | | -3 | | 4 | |
| **Changes in mean sea level, relative to global average mean sea level rise (m)** | | | | | | | |
| 0 to 0.04 | | 0.04 to 0.08 | | 0 to 0.04 | | 0.08 to 0.12 | |

***Table S2***: *Summary of climate change projections for Batemans Bay for 2030 and 2070 derived from the CCM2 and CCM3 simulations. Changes in mean sea level are relative to global average mean sea level rise, which is projected to be 0.18 to 0.79m by 2095, relative to the global average mean sea level for 1990. Other changes are relative to climatological averages for 1990. Unsigned numbers in red indicate increases. Numbers in blue indicate decreases. Source: Holper et al. (2006) and McInnes et al. (2007).*

| 2030 | | | | 2070 | | | |
|---|---|---|---|---|---|---|---|
| CCM2 Low GW | CCM2 High GW | CCM3 Low GW | CCM3 High GW | CCM2 Low GW | CCM2 High GW | CCM3 Low GW | CCM3 High GW |
| **Changes in annual average daily maximum air temperatures (°C)** | | | | | | | |
| 0.5 | 1.1 | 0.7 | 1.5 | 1.1 | 3.4 | 1.4 | 4.6 |
| **Changes in annual average daily minimum air temperatures (°C)** | | | | | | | |
| 0.4 | 1.0 | 0.6 | 1.4 | 1.0 | 3.1 | 1.3 | 4.3 |
| **Changes in annual average rainfall totals (%)** | | | | | | | |
| -3 | -8 | 4 | 10 | -7 | -23 | 9 | 30 |
| **Changes in annual average solar radiation (%)** | | | | | | | |
| 0.1 | 0.2 | 0.1 | 0.3 | 0.2 | 0.6 | 0.3 | 0.8 |
| **CCM2** | | **CCM3** | | **CCM2** | | **CCM3** | |
| **Annual dominant wind direction** | | | | | | | |
| SW (202.5 to 247.5°) | | | | | | | |
| **Changes in the frequency of annual dominant wind direction days with average wind speeds greater than 8m/s (%)** | | | | | | | |
| -1 | | 2 | | -2 | | 8 | |
| **Changes in the 1-in-100 year storm surge height (%)** | | | | | | | |
| -1 | | 1 | | -3 | | 1 | |
| **Changes in mean sea level, relative to global average mean sea level rise (m)** | | | | | | | |
| 0 to 0.04 | | 0 to 0.04 | | 0 to 0.04 | | 0.08 to 0.12 | |

***Table S3:*** *Summary of climate change projections for rainfall extremes for the Wooli Wooli Estuary and Batemans Bay for 2030 and 2070. Changes in the intensity of extreme rainfall events are relative to the climate of 1980. Source: Hennessy et al. (2004) and Mpelasoka et al. (2007).*

| Location | 2030 | 2070 |
|---|---|---|
| **Changes in the intensity of extreme rainfall events analysed on an annual basis (%)** | | |
| Wooli Wooli Estuary | -10 to 0 | -10 to +10 |
| Batemans Bay | -10 to +10 | -10 to 0 |
| **Drought frequency (% of months per decade)** | | |
| Southeast Coast Drainage Division | < 24 | < 28 |

# 1. INTRODUCTION

Communities and assets along the New South Wales (NSW) coastline will increasingly come under threat from a range of climate change impacts. These include coastal flooding and erosion due to rising mean sea levels and possible changes in weather patterns that drive sea level extremes such as storm surges. In addition, estuaries along the NSW coast may also suffer from increased flooding during extreme events and lower overall flows leading to water supply and quality issues.

The aim of this report is to describe how the variables that influence estuarine response may change as a result of climate change due to the enhanced greenhouse effect for the 2030 and 2070 planning horizons. Two study locations have been selected. The first location is the Wooli Wooli River system on the NSW north coast (see Figure 1), which is a barrier estuary. The second is the Clyde River/Batemans Bay system on the NSW south coast (see Figure 1), which is a drowned river valley. It is envisaged that the study of these two very different estuary systems will facilitate the assessment of the impacts of climate change on other estuaries on the NSW coast.

This report complements a report by McInnes et al. (2007) that investigated how environmental variables that influence coastal erosion at the Wooli Wooli Estuary and Batemans Bay may change as a result of climate change due to the enhanced greenhouse effect for the 2030 and 2070 planning horizons. It draws on the McInnes et al. (2007) report and other existing literature to provide projections of changes in average temperature, rainfall and solar radiation, wind conditions, storm surge heights, mean sea level, extreme rainfall events and drought frequency for the same two locations and planning horizons.

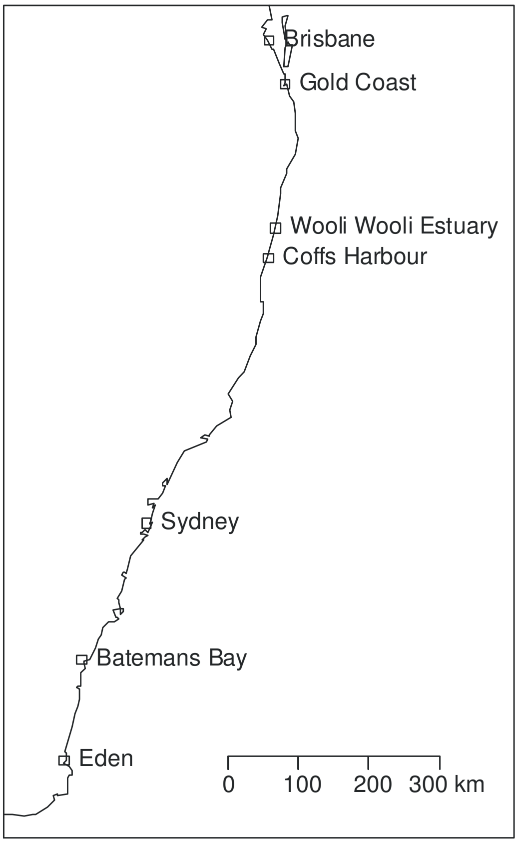


***Figure 1:*** *The locations of the Wooli Wooli Estuary and Batemans Bay on the New South Wales coast.*

# 2. METHODS FOR PRODUCING CLIMATE PROJECTIONS

## 2.1. Uncertainty in Regional Climate Change

There are three main sources of uncertainty to be considered when producing projections of global warming-induced climate change for a region for a given year in the future:

1) The uncertainty in the future evolution of greenhouse gas concentrations in the atmosphere.

2) The uncertainty in how much the global average surface temperature will respond to increases in atmospheric greenhouse gas concentrations.

3) The uncertainty in how changes to the climate as a result of global warming will vary spatially and hence how the climate of the region under consideration will respond to an increase in global average surface temperature.

The first uncertainty can be addressed by considering different plausible storylines of future global demographic, economic and technological change. The Intergovernmental Panel on Climate Change's Special Report on Emission Scenarios (SRES) (IPCC, 2000) has provided greenhouse gas emission scenarios associated with a suite of such storylines. The second uncertainty can be addressed by considering the future rates of future global warming in simulations of different climate models forced with increases in atmospheric greenhouse gas concentrations arising from the SRES emission scenarios. Figure 2 illustrates how consideration of the first two uncertainties can yield a range of likely global warming values for a given year. The light grey area depicts the envelope of likely changes in global average surface temperature, relative to the climatological average for 1990, when the responses of an ensemble of climate models to increases in atmospheric greenhouse gas concentrations arising from the SRES emission scenarios are considered. The lower and upper edges of the light grey area can be regarded as defining global warming values for low-end and high-end global warming scenarios, respectively. Table 1 shows such global warming values for low-end and high-end global warming scenarios for the years 2030 and 2070 derived from the data underlying Figure 2 published in the Third Assessment Report of the Intergovernmental Panel on Climate Change (IPCC, 2001).

***Table 1:*** *Global warming values (*°C*) for low-end and high-end global warming scenarios for 2030 and 2070, relative to the climatological global average surface temperature for 1990. Source: IPCC (2001).*

| 2030 | | 2070 | |
|---|---|---|---|
| Low | High | Low | High |
| 0.54 | 1.24 | 1.17 | 3.77 |

The third uncertainty, the uncertainty in the response of the regional climate to a given global warming value, can be addressed by considering the response of the climate of the region of interest to global warming in multiple climate models.

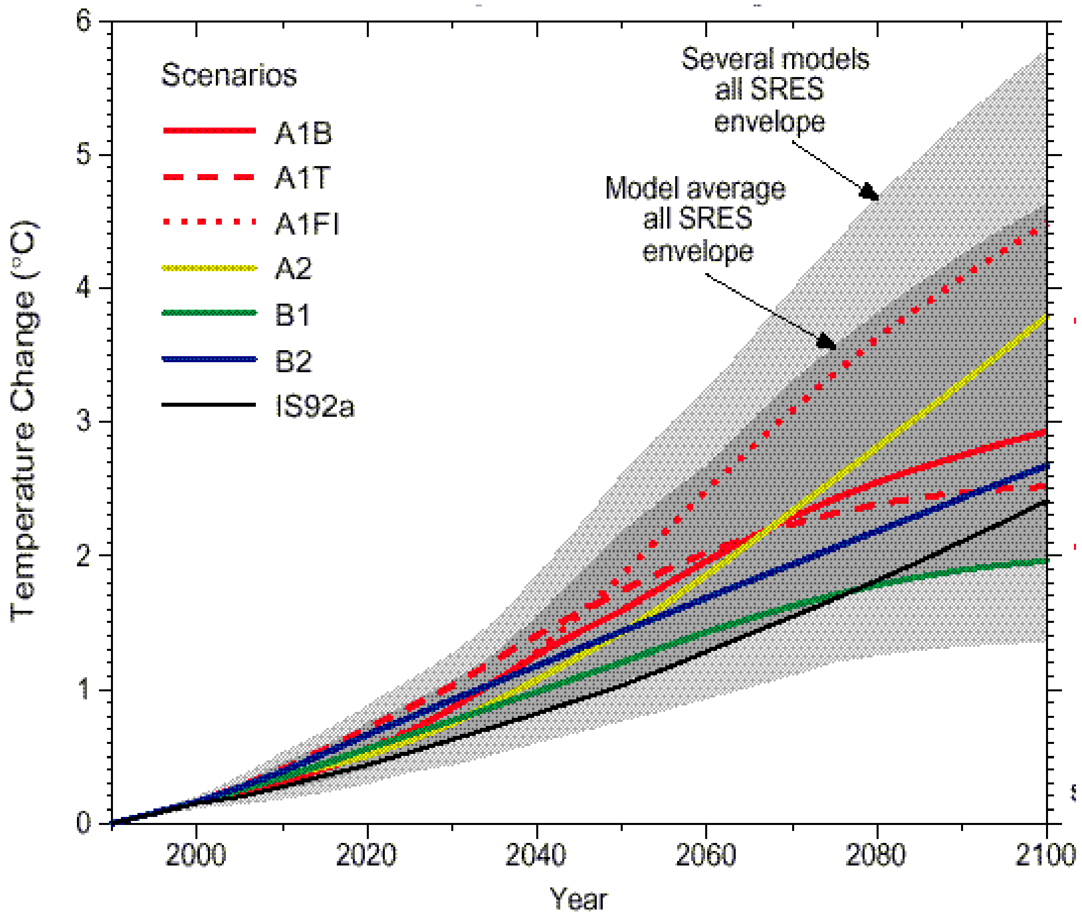


***Figure 2:*** *Changes in global average surface temperature for the 21st Century, relative to the climatological average for 1990. The coloured lines indicate changes based on the average response of an ensemble of climate models to a subset of the SRES emission scenarios. The dark grey area depicts changes based on the response of the average of the ensemble of models to the full set of SRES emission scenarios. The light grey area depicts changes based on the response of the ensemble to the full set of emission scenarios. Source: IPCC (2001).*

## 2.2. Climate Model Simulations

Most of the climate change projections in the McInnes et al. (2007) report were based on the output of two climate model configurations involving CSIRO's Cubic Conformal Atmospheric Model (CCAM) (see McGregor and Dix, 2001 and McGregor, 2005). In this report, where they have been available, projections derived from the same two model configurations have been presented in order to describe climate change scenarios that are consistent with the information from the McInnes et al. (2007) report.

CCAM has a grid that covers the entire globe but the resolution of the grid is spatially variable. In the climate model simulations used by McInnes et al. (2007) the model is configured such that the resolution of the grid is fine, representing spatial scales of around 60km, over Australia and coarser elsewhere. In the coarse parts of the grid, in which atmospheric processes are least well represented, adjustments to CCAM simulations are applied based on the output of a model with a more uniform grid. The work of McInnes et al. (2007) was based on two CCAM simulations, one constrained using output of the CSIRO Mark2 model (see Hirst et al., 2000) and one constrained using output of the CSIRO Mark3 model (see Gordon et al., 2002). The simulations, hereafter referred to in this report as

“CCM2” and “CCM3” were forced with historical atmospheric greenhouse gas concentrations until 1990 and with the mid to high estimates of future atmospheric greenhouse gas concentrations arising from the SRES A2 emission scenario described in IPCC (2000) from then on. The SRES A2 emission scenario, under which atmospheric carbon dioxide concentrations rise from their present level of about 370ppm to about 880ppm by 2100, yields approximately mid-range values of global warming (see Figure 2).

Table 2 summarises the climate model simulations used by McInnes et al. (2007).

***Table 2:*** *Climate model simulations used by McInnes et al. (2007).*

| Simulation | Emission scenario | Source of adjustments in coarse parts of grid | Finest spatial scale represented |
|---|---|---|---|
| Mark2 | SRES A2 | - | ~400km |
| Mark3 | SRES A2 | - | ~200km |
| CCM2 | SRES A2 | Mark2 | ~60km |
| CCM3 | SRES A2 | Mark3 | ~60km |

# 3. AVERAGE TEMPERATURE, RAINFALL AND SOLAR RADIATION

For average temperature, rainfall and solar radiation it has been possible to present projections that sample the uncertainty in the future rate of global warming by combining the CCM2 and CCM3 responses of the regional climate to global warming with global warming values for low-end and high-end global warming scenarios (see Table 1). These were obtained from data underlying a study of the impacts of climate change on infrastructure in Victoria (Holper et al., 2006). Following the “pattern scaling” method described by Whetton et al. (2007), Holper et al. (2006) derived Australia-wide patterns of change in various climate variables per °C of global warming for CCM2 and CCM3. These were scaled by the global warming values for low-end and high-end global warming scenarios in Table 1 to produce projections of changes for 2030 and 2070. This combination of the two different model responses of the regional climate to global warming with global warming values for low-end and high-end global warming scenarios yielded four scenarios of regional climate change for each of the years of interest (see Table 3).

***Table 3:*** *Scenarios of regional climate change considered by Holper et al. (2006).*

| Scenario | Description |
|---|---|
| **CCM2 Low GW** | Regional climate response to global warming of **CCM2** combined with the **low**-end value of the likely increase in global average temperature. |
| **CCM2 High GW** | Regional climate response to global warming of **CCM2** combined with the **high**-end value of the likely increase in global average temperature. |
| **CCM3 Low GW** | Regional climate response to global warming of **CCM3** combined with the **low**-end value of the likely increase in global average temperature. |
| **CCM3 High GW** | Regional climate response to global warming of **CCM3** combined with the **high**-end value of the likely increase in global average temperature. |

Tables 4 and 5 show projected changes in annual and seasonal average air temperatures, rainfall totals and solar radiation for the Wooli Wooli Estuary and Batemans Bay extracted from the Holper et al. (2006) data. Projections of changes in annual and seasonal average values of daily maximum air temperature and daily minimum air temperature were obtained. The rainfall changes given are changes in the total quantity of rain falling on a unit area of the Earth’s surface over a year and over each season. The solar radiation changes given are changes in the energy transferred to a unit area of the Earth’s surface by incoming shortwave electromagnetic radiation from the Sun over a year and over each season. By this definition, solar radiation is a gross quantity not directly dependent on the rate of energy transfer from the surface by outgoing reflected shortwave radiation and re-radiated longwave radiation.

***Table 4:*** *Changes in annual and seasonal average climate conditions for the Wooli Wooli Estuary for 2030 and 2070, relative to climatological averages for 1990. Unsigned numbers in red indicate increases. Numbers in blue indicate decreases. Source: Holper et al. (2006).*

| Season | 2030 | | | | 2070 | | | |
|---|---|---|---|---|---|---|---|---|
| | CCM2 Low GW | CCM2 High GW | CCM3 Low GW | CCM3 High GW | CCM2 Low GW | CCM2 High GW | CCM3 Low GW | CCM3 High GW |
| **Changes in average daily maximum air temperatures (℃)** | | | | | | | | |
| Annual | 0.5 | 1.2 | 0.6 | 1.3 | 1.1 | 3.6 | 1.2 | 4.0 |
| Summer | 0.6 | 1.4 | 0.6 | 1.3 | 1.3 | 4.2 | 1.3 | 4.1 |
| Autumn | 0.5 | 1.0 | 0.5 | 1.2 | 1.0 | 3.2 | 1.1 | 3.6 |
| Winter | 0.5 | 1.1 | 0.6 | 1.4 | 1.0 | 3.4 | 1.3 | 4.3 |
| Spring | 0.6 | 1.3 | 0.6 | 1.3 | 1.2 | 3.9 | 1.2 | 4.0 |
| **Changes in average daily minimum air temperatures (℃)** | | | | | | | | |
| Annual | 0.5 | 1.1 | 0.6 | 1.3 | 1.1 | 3.5 | 1.2 | 4.0 |
| Summer | 0.5 | 1.2 | 0.5 | 1.2 | 1.1 | 3.7 | 1.1 | 3.6 |
| Autumn | 0.5 | 1.1 | 0.5 | 1.2 | 1.0 | 3.3 | 1.1 | 3.6 |
| Winter | 0.4 | 1.0 | 0.7 | 1.6 | 1.0 | 3.1 | 1.5 | 4.9 |
| Spring | 0.6 | 1.3 | 0.6 | 1.3 | 1.2 | 3.8 | 1.2 | 3.9 |
| **Changes in average rainfall totals (%)** | | | | | | | | |
| Annual | -3 | -6 | 0 | 0 | -6 | -19 | 0 | -1 |
| Summer | -4 | -9 | -3 | -7 | -8 | -27 | -6 | -20 |
| Autumn | -2 | -5 | 0 | 0 | -5 | -15 | 0 | 1 |
| Winter | -4 | -9 | 4 | 8 | -8 | -27 | 8 | 25 |
| Spring | -1 | -2 | 0 | 0 | -2 | -7 | 0 | -1 |
| **Changes in average solar radiation (%)** | | | | | | | | |
| Annual | 0.3 | 0.6 | 0.2 | 0.5 | 0.6 | 1.8 | 0.5 | 1.6 |
| Summer | 0.5 | 1.2 | 0.4 | 1.0 | 1.1 | 3.5 | 0.9 | 3.0 |
| Autumn | 0.0 | 0.0 | 0.1 | 0.2 | 0.0 | 0.0 | 0.2 | 0.6 |
| Winter | 0.8 | 1.7 | -0.3 | -0.8 | 1.6 | 5.3 | -0.7 | -2.3 |
| Spring | -0.1 | -0.2 | 0.4 | 0.9 | -0.2 | -0.7 | 0.9 | 2.9 |

***Table 5:*** *Changes in annual and seasonal average climate conditions for Batemans Bay for 2030 and 2070, relative to climatological averages for 1990. Unsigned numbers in red indicate increases. Numbers in blue indicate decreases. Source: Holper et al. (2006).*

| Season | 2030 | | | | 2070 | | | |
|---|---|---|---|---|---|---|---|---|
| | CCM2 Low GW | CCM2 High GW | CCM3 Low GW | CCM3 High GW | CCM2 Low GW | CCM2 High GW | CCM3 Low GW | CCM3 High GW |
| **Changes in average daily maximum air temperatures (°C)** | | | | | | | | |
| Annual | 0.5 | 1.1 | 0.7 | 1.5 | 1.1 | 3.4 | 1.4 | 4.6 |
| Summer | 0.5 | 1.1 | 0.7 | 1.5 | 1.1 | 3.5 | 1.4 | 4.6 |
| Autumn | 0.4 | 1.0 | 0.6 | 1.3 | 0.9 | 2.9 | 1.2 | 3.9 |
| Winter | 0.5 | 1.1 | 0.7 | 1.6 | 1.0 | 3.4 | 1.5 | 4.9 |
| Spring | 0.6 | 1.3 | 0.7 | 1.6 | 1.2 | 4.0 | 1.5 | 4.9 |
| **Changes in average daily minimum air temperatures (°C)** | | | | | | | | |
| Annual | 0.4 | 1.0 | 0.6 | 1.4 | 1.0 | 3.1 | 1.3 | 4.3 |
| Summer | 0.5 | 1.1 | 0.6 | 1.4 | 1.0 | 3.3 | 1.4 | 4.4 |
| Autumn | 0.4 | 1.0 | 0.6 | 1.3 | 0.9 | 3.0 | 1.2 | 3.9 |
| Winter | 0.4 | 0.9 | 0.7 | 1.5 | 0.9 | 2.8 | 1.4 | 4.6 |
| Spring | 0.5 | 1.1 | 0.6 | 1.4 | 1.1 | 3.4 | 1.3 | 4.2 |
| **Changes in average rainfall totals (%)** | | | | | | | | |
| Annual | -3 | -8 | 4 | 10 | -7 | -23 | 9 | 30 |
| Summer | -2 | -6 | 1 | 2 | -5 | -17 | 2 | 6 |
| Autumn | 0 | 0 | 8 | 19 | 0 | -1 | 18 | 57 |
| Winter | -7 | -15 | 9 | 20 | -14 | -46 | 19 | 62 |
| Spring | -4 | -9 | -1 | -2 | -9 | -29 | -2 | -6 |
| **Changes in average solar radiation (%)** | | | | | | | | |
| Annual | 0.1 | 0.2 | 0.1 | 0.3 | 0.2 | 0.6 | 0.3 | 0.8 |
| Summer | -0.1 | -0.3 | 0.2 | 0.4 | -0.2 | -0.8 | 0.4 | 1.3 |
| Autumn | -0.1 | -0.3 | 0.2 | 0.5 | -0.3 | -0.8 | 0.4 | 1.4 |
| Winter | 0.7 | 1.6 | -0.4 | -0.9 | 1.5 | 4.9 | -0.8 | -2.6 |
| Spring | 0.1 | 0.3 | 0.2 | 0.5 | 0.3 | 0.9 | 0.5 | 1.6 |

# 4. WIND CONDITIONS

McInnes et al. (2007) used the CCM2 and CCM3 simulations to investigate changes in broad scale wind conditions for oceanic regions near the Wooli Wooli Estuary (153-158°E, 29-33°S) and Batemans Bay (150-155°E, 34-39°S). The pattern scaling method of producing climate change projections used by Holper et al. (2006) was not employed and the analysis was based directly on the output of the simulations. Hence two scenarios of regional climate change, arising from the two different model responses of the regional climate to the SRES A2 emission scenario, were considered. A frequency analysis in which daily average winds for each season of the year and for the whole seasonal cycle were binned into eight 45° directional sectors and five wind speed classes was performed for three 40 year periods centred on 1980, 2030 and 2070.

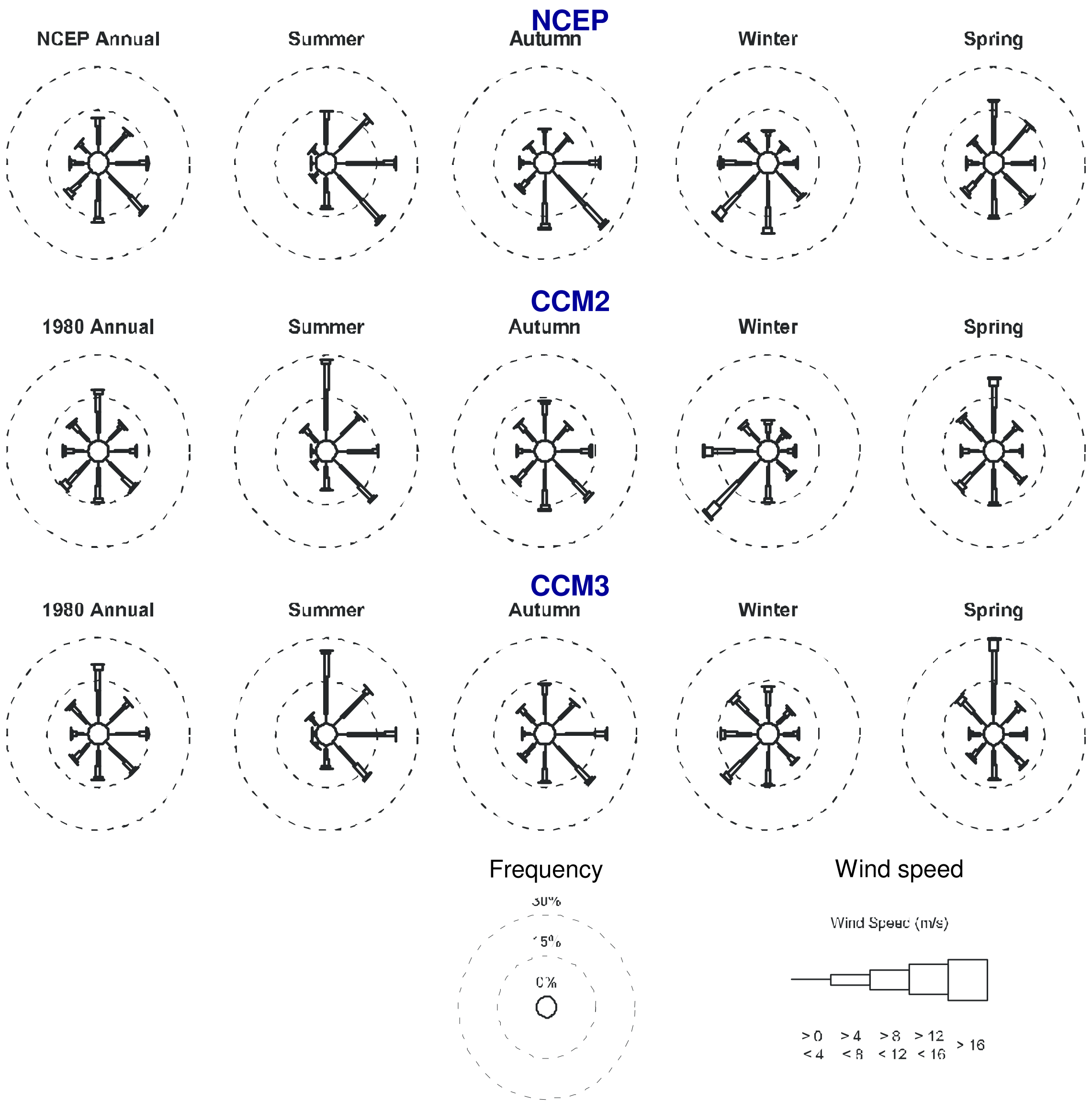


***Figure 3:*** *Annual and seasonal wind roses for the ocean near the Wooli Estuary (153-158°E, 29-33°S) for a 40 year period centred on 1980. Source: McInnes et al. (2007).*

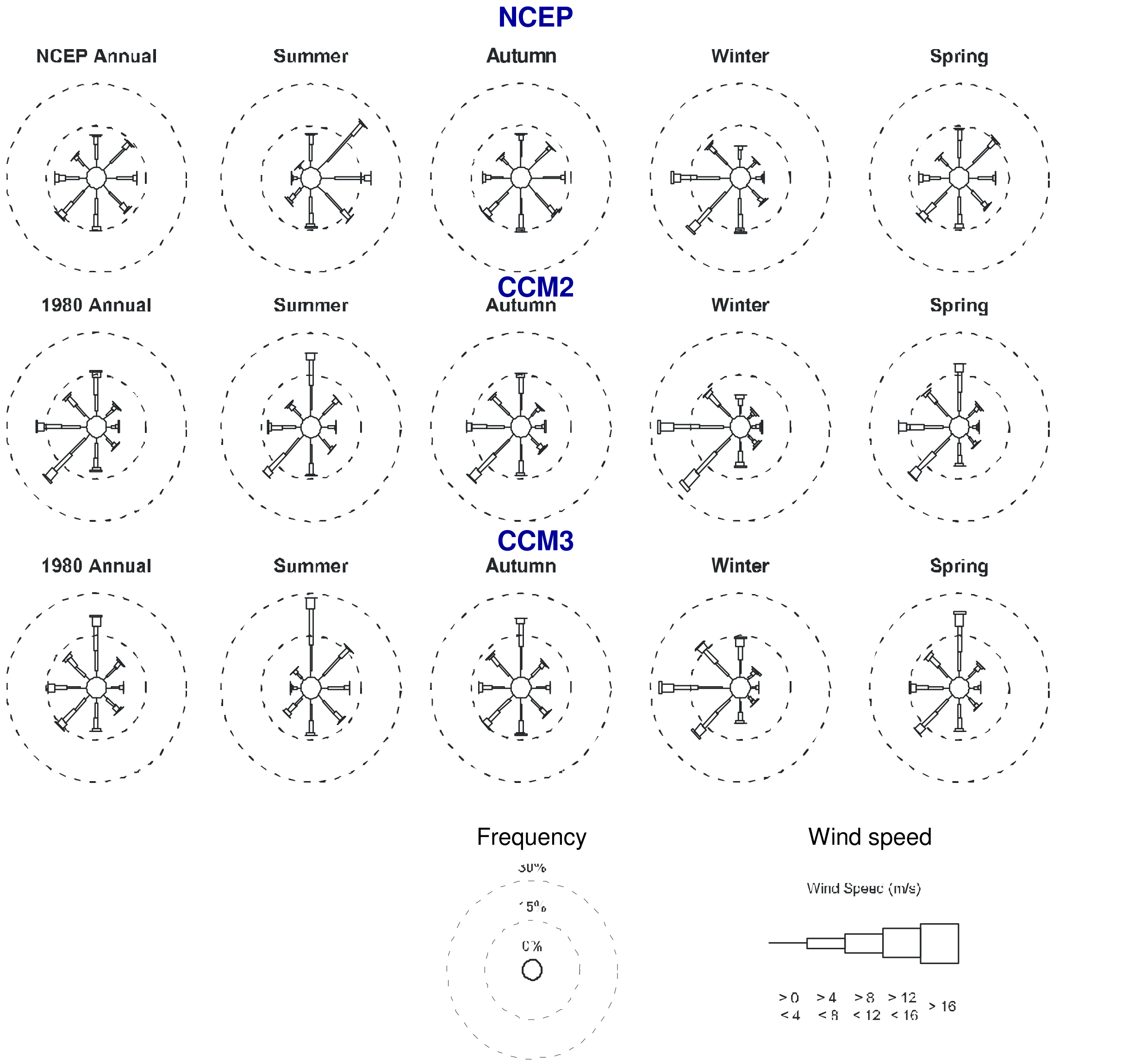


***Figure 4:*** *Annual and seasonal wind roses for the ocean near Batemans Bay (150-155°E, 34-39°S) for a 40 year period centred on 1980. Source: McInnes et al. (2007).*

The frequency distributions derived from the CCM2 and CCM3 simulations for the climate of 1980 were compared with corresponding distributions derived from the National Center for Environmental Prediction (NCEP) reanalysis data set (Kalnay et al., 1996), representing distributions based on observations of wind conditions. Figures 3 and 4 show distributions for the ocean near the Wooli Wooli Estuary and Batemans Bay for 1980 derived from CCM2, CCM3 and the NCEP reanalysis data set. It should be noted that the McInnes et al. (2007) analysis was of broad scale wind conditions over 5° boxes covering the ocean near the Wooli Wooli Estuary and Batemans Bay. Therefore the distributions shown in Figures 3 and 4 do not represent the localised wind conditions that would be measured at meteorological observing stations sited at each location.

There are some systematic differences between the distributions derived from the simulations and those from the reanalysis data set. For example, for both locations, there is a higher frequency of winds from the north in the CCM2 output than in the reanalysis data set. For both locations, there is a higher frequency of northerly winds in all seasons in the CCM3 output than in the reanalysis data set. To avoid any influence of such model biases on subsequent impact studies, McInnes et al. (2007)

focussed on differences between the distributions derived from the simulations for 1980 and each of 2030 and 2070, assuming that the differences were robust even though the 1980 distributions from the simulations differed from the corresponding distributions from the reanalysis data set. Here, we adopt the same philosophy.

The frequency distributions for 1980 from the NCEP reanalysis data set shown in Figures 3 and 4 were used as the basis of projections of wind conditions for 2030 and 2070. The 45° directional resolution of the analysis was too coarse to provide evidence of future changes in the most common wind direction, hereafter referred to in this report as "the dominant wind direction", on an annual basis or for any season for either location, suggesting that any changes in annual or seasonal dominant wind directions in the simulations were less than 45°. For each simulation and location, the changes in the frequency distribution of the speeds of winds from the dominant wind direction were assessed on an annual basis and for each season for 2030 and 2070. Percentage changes in the frequency of the speeds of winds from the dominant wind direction for each of the five wind speed classes were calculated. These were then applied to the corresponding distribution for 1980 from the NCEP reanalysis data set. The resulting annual and seasonal frequency distributions of the speeds of winds from the dominant wind direction for 2030 and 2070 are shown in Tables 6 and 7.

***Table 6:*** *Annual and seasonal frequency distributions of the speeds of winds from the dominant wind direction for the ocean near the Wooli Wooli Estuary (153-158°E, 29-33°S) for 1980, 2030 and 2070. Source: McInnes et al. (2007).*

| Season | 1980 | 2030 | | 2070 | |
|---|---|---|---|---|---|
| | NCEP | CCM2 | CCM3 | CCM2 | CCM3 |
| **Dominant wind direction** | | | | | |
| Annual | SE (112.5 to 157.5°) | | | | |
| Summer | SE (112.5 to 157.5°) | | | | |
| Autumn | SE (112.5 to 157.5°) | | | | |
| Winter | S (157.5 to 202.5°) | | | | |
| Spring | N (337.5 to 22.5°) | | | | |
| **Dominant wind directions days with average wind speeds less than 4m/s (%)** | | | | | |
| Annual | 13 | 14 | 13 | 14 | 13 |
| Summer | 11 | 10 | 12 | 11 | 10 |
| Autumn | 11 | 13 | 11 | 12 | 12 |
| Winter | 13 | 14 | 12 | 14 | 14 |
| Spring | 16 | 15 | 16 | 16 | 16 |
| **Dominant wind directions days with average wind speeds between 4 and 8m/s (%)** | | | | | |
| Annual | 52 | 53 | 50 | 54 | 49 |
| Summer | 49 | 46 | 47 | 49 | 47 |
| Autumn | 52 | 56 | 49 | 56 | 50 |
| Winter | 42 | 39 | 41 | 37 | 39 |
| Spring | 53 | 53 | 53 | 53 | 52 |
| **Dominant wind directions days with average wind speeds between 8 and 12m/s (%)** | | | | | |
| Annual | 31 | 30 | 33 | 30 | 33 |
| Summer | 37 | 39 | 37 | 36 | 38 |
| Autumn | 33 | 29 | 36 | 30 | 32 |
| Winter | 35 | 35 | 35 | 37 | 35 |
| Spring | 28 | 29 | 28 | 28 | 28 |
| **Dominant wind directions days with average wind speeds between 12 and 16m/s (%)** | | | | | |
| Annual | 3 | 3 | 4 | 3 | 4 |
| Summer | 3 | 5 | 5 | 3 | 5 |
| Autumn | 3 | 2 | 4 | 2 | 4 |
| Winter | 9 | 11 | 11 | 10 | 11 |
| Spring | 3 | 3 | 4 | 3 | 4 |
| **Dominant wind directions days with average wind speeds greater than 16m/s (%)** | | | | | |
| Annual | 0 | 0 | 0 | 0 | 0 |
| Summer | 0 | 0 | 0 | 0 | 0 |
| Autumn | 0 | 0 | 0 | 0 | 2 |
| Winter | 1 | 1 | 2 | 1 | 1 |
| Spring | 0 | 0 | 0 | 0 | 0 |

*Table 7: Annual and seasonal frequency distributions of the speeds of winds from the dominant wind direction for the ocean near Batemans Bay (150-155°E, 34-39°S) for 1980, 2030 and 2070. Source: McInnes et al. (2007).*

| Season | 1980 | 2030 | | 2070 | |
|---|---|---|---|---|---|
| | NCEP | CCM2 | CCM3 | CCM2 | CCM3 |
| **Dominant wind direction** | | | | | |
| Annual | SW (202.5 to 247.5°) | | | | |
| Summer | NE (22.5 to 67.5°) | | | | |
| Autumn | S (157.5 to 202.5°) | | | | |
| Winter | SW (202.5 to 247.5°) | | | | |
| Spring | SW (202.5 to 247.5°) | | | | |
| **Dominant wind directions days with average wind speeds less than 4m/s (%)** | | | | | |
| Annual | 19 | 20 | 19 | 20 | 17 |
| Summer | 20 | 19 | 21 | 19 | 21 |
| Autumn | 23 | 23 | 21 | 24 | 20 |
| Winter | 16 | 15 | 16 | 15 | 14 |
| Spring | 20 | 21 | 20 | 22 | 19 |
| **Dominant wind directions days with average wind speeds between 4 and 8m/s (%)** | | | | | |
| Annual | 37 | 37 | 37 | 37 | 35 |
| Summer | 56 | 56 | 57 | 57 | 57 |
| Autumn | 37 | 38 | 34 | 37 | 32 |
| Winter | 36 | 36 | 36 | 36 | 35 |
| Spring | 37 | 36 | 35 | 37 | 34 |
| **Dominant wind directions days with average wind speeds between 8 and 12m/s (%)** | | | | | |
| Annual | 29 | 28 | 29 | 28 | 29 |
| Summer | 22 | 23 | 21 | 22 | 20 |
| Autumn | 28 | 27 | 28 | 28 | 29 |
| Winter | 30 | 30 | 30 | 29 | 30 |
| Spring | 28 | 28 | 29 | 28 | 30 |
| **Dominant wind directions days with average wind speeds between 12 and 16m/s (%)** | | | | | |
| Annual | 13 | 13 | 13 | 13 | 15 |
| Summer | 1 | 2 | 1 | 2 | 1 |
| Autumn | 10 | 10 | 14 | 10 | 16 |
| Winter | 15 | 16 | 16 | 16 | 17 |
| Spring | 13 | 13 | 13 | 11 | 14 |
| **Dominant wind directions days with average wind speeds greater than 16m/s (%)** | | | | | |
| Annual | 2 | 2 | 2 | 2 | 3 |
| Summer | 0 | 0 | 0 | 0 | 0 |
| Autumn | 2 | 2 | 3 | 2 | 3 |
| Winter | 3 | 3 | 3 | 3 | 5 |
| Spring | 2 | 2 | 2 | 2 | 3 |

# 5. PROJECTIONS OF SEA LEVELS

## 5.1. Storm Surge Heights

Storm surges are events in which coastal sea levels are elevated above the level of the predicted tide due to strong winds and falling atmospheric pressure associated with severe weather systems. McInnes et al. (2007) used the output of the CCM2 and CCM3 simulations to investigate changes in storm surges for the Wooli Wooli Estuary and Batemans Bay. Return levels for storm surge height, the height of the sea level above the level of the predicted tide, were estimated for the current climate and the climates of 2030 and 2070. The pattern scaling method of producing climate change projections used by Holper et al. (2006) was not employed and the analysis was based directly on the output of the simulations. Hence two scenarios of regional climate change, arising from the two different simulated responses of the regional climate to the SRES A2 emission scenario, were considered.

Table 8 shows storm surge height return levels for the Wooli Wooli Estuary and Batemans Bay for the current climate and for 2030 and 2070. 95% confidence intervals associated with the extreme value analysis used to estimate the return levels are also shown. Future decreases in the frequencies of storms suggested by CCM2 are associated with 0.01 to 0.02m decreases in storm surge height return levels. Future increases in the frequencies of storms suggested by CCM3 are associated with 0.01 to 0.03m increases in storm surge height return levels. For both the Wooli Wooli Estuary and Batemans Bay, the future storm surge height return levels lie within the range defined by the 95% confidence intervals for the corresponding current climate return levels. However, since the future return levels were derived from the current climate return levels, the estimates of the two sets of levels are not independent, meaning that the conclusion that there are no statistically significant changes in storm surge height cannot be drawn from Table 8.

***Table 8:*** *Storm surge height return levels for the Wooli Wooli Estuary and Batemans Bay for the current climate and for 2030 and 2070 with 95% confidence intervals associated with extreme value analysis. Source: McInnes et al. (2007).*

| Return period | Current climate | 2030 | | 2070 | |
|---|---|---|---|---|---|
| | | CCM2 | CCM3 | CCM2 | CCM3 |
| **Storm surge height return levels for the Wooli Wooli Estuary (m)** | | | | | |
| 10yr | 0.48 ± 0.06 | 0.48 ± 0.06 | 0.49 ± 0.06 | 0.47 ± 0.05 | 0.51 ± 0.07 |
| 20yr | 0.53 ± 0.08 | 0.53 ± 0.08 | 0.54 ± 0.09 | 0.52 ± 0.07 | 0.56 ± 0.10 |
| 50yr | 0.61 ± 0.12 | 0.60 ± 0.12 | 0.62 ± 0.13 | 0.59 ± 0.11 | 0.64 ± 0.14 |
| 100yr | 0.67 ± 0.16 | 0.66 ± 0.16 | 0.68 ± 0.17 | 0.65 ± 0.15 | 0.70 ± 0.19 |
| **Storm surge height return levels for Batemans Bay (m)** | | | | | |
| 10yr | 0.57 ± 0.08 | 0.57 ± 0.07 | 0.58 ± 0.08 | 0.55 ± 0.07 | 0.59 ± 0.09 |
| 20yr | 0.61 ± 0.10 | 0.61 ± 0.10 | 0.62 ± 0.11 | 0.60 ± 0.09 | 0.63 ± 0.11 |
| 50yr | 0.66 ± 0.13 | 0.66 ± 0.13 | 0.67 ± 0.14 | 0.65 ± 0.12 | 0.68 ± 0.14 |
| 100yr | 0.70 ± 0.16 | 0.69 ± 0.15 | 0.71 ± 0.17 | 0.68 ± 0.15 | 0.71 ± 0.17 |

## 5.2. Mean Sea Level

Relative to the 1990 level, global average mean sea level is likely to increase by 0.18 to 0.59m by 2095, with potentially an additional contribution from a future rapid dynamical response of the ice sheets of possibly 0.1 to 0.2m (IPCC, 2007). However, increases in sea level will not occur uniformly across the globe with some regions experiencing higher levels of sea level rise than others. Such variations are due to variations in the thermal expansion of the ocean.

McInnes et al. (2007) used output of the CSIRO Mark2 and CSIRO Mark3 climate model simulations used to constrain the CCM2 and CCM3 simulations in the coarse parts of their grids, described in Table 2, to provide estimates of the component of mean sea level rise due to thermal expansion in the vicinities of the Wooli Wooli Estuary and Batemans Bay. The pattern scaling method of producing climate change projections used by Holper et al. (2006) was not employed and the analysis was based directly on the output of the Mark2 and Mark3 simulations. Hence two scenarios of regional climate change, arising from the two different simulated responses of the regional climate to the SRES A2 emission scenario, were considered. Since the output of the Mark2 and Mark3 simulations were used to provide oceanic boundary conditions for the CCM2 and CCM3 simulations, the mean sea level rise estimates for these scenarios can be regarded as being consistent with the scenarios arising from the CCM2 and CCM3 responses of the regional climate to the SRES A2 emission scenario. They are therefore labelled “CCM2” and “CCM3” in Table 9.

***Table 9:*** *Mean sea level rise due to thermal expansion (m) for Wooli Wooli Estuary and Batemans Bay for 2030 and 2070, relative to global average mean sea level rise. Source: McInnes et al. (2007).*

| Location | 2030 | | 2070 | |
|---|---|---|---|---|
| | CCM2 | CCM3 | CCM2 | CCM3 |
| Wooli Wooli Estuary | 0 to 0.04 | 0.04 to 0.08 | 0 to 0.04 | 0.08 to 0.12 |
| Batemans Bay | 0 to 0.04 | 0 to 0.04 | 0 to 0.04 | 0.08 to 0.12 |

# 6. PROJECTIONS OF RAINFALL EXTREMES

## 6.1. Extreme Rainfall Events

Projections of changes in the intensity of extreme rainfall events for the Wooli Wooli Estuary and Batemans Bay were obtained from a study of projected changes in climate extremes in NSW by Hennessy et al. (2004). Hennessy et al. (2004) derived projections of the intensity of extreme rainfall events for 2030 and 2070 from simulations of four different CSIRO climate model simulations, including CCM2 but not including CCM3 (see Table 10). Each model was forced with historical atmospheric greenhouse gas concentrations until 1990 and with either the mid-range estimates of future atmospheric greenhouse gas concentrations arising from the Intergovernmental Panel on Climate Change's IS92a emission scenario (see IPCC, 2000) or the mid to high estimates of future concentrations arising from the SRES A2 emission scenario from then on.

***Table 10:*** *Climate model simulations used by Hennessy et al. (2004) for an analysis of extreme rainfall events.*

| Simulation | Emission scenario | Post-1990 atmospheric greenhouse gas forcing | Finest spatial scale represented |
|---|---|---|---|
| Mark2 | IS92a | Mid-range | ~400km |
| DARLAM | IS92a | Mid-range | ~125km |
| Mark3 | SRES A2 | Mid to high | ~200km |
| CCM2 | SRES A2 | Mid to high | ~60km |

The output of all four simulations was interpolated to a common grid with a resolution of approximately 50km and the data for each grid point in NSW were analysed separately. For each model simulation, the four greatest daily rainfall accumulations, corresponding to 1-in-40 year, 1-in-20 year, 1-in-10 year and 1-in-5 year accumulations, were identified in each of three 40 year periods centred on 1980, 2030 and 2070. Fractional changes in the intensity of extreme rainfall events for each return period were calculated for the climates of 2030 and 2070, relative to the climate of 1980, for each simulation. These were averaged across return periods to give a single change for each of the four simulations for each of 2030 and 2070. Finally, the four changes for each of 2030 and 2070 were averaged to give a single change for the whole set of simulations for each year. Table 11 shows projected changes in the intensity of extreme rainfall events for the grid points in the vicinities of Wooli Wooli Estuary and Batemans Bay. Ranges of approximate change are presented to represent the variability in changes between grid points.

The results shown in Table 11 should be used with caution as they are based on an analysis of the output of climate models in which fine scale features of terrain and weather systems, important drivers of extreme rainfall events, are not well represented. It is possible that there will be local increases in the intensity of extreme rainfall events within the vicinities of Wooli Wooli Estuary and Batemans Bay for seasons in future climates for which decreases are indicated.

***Table 11:*** *Changes (%) in the intensity of extreme rainfall events for the Wooli Wooli Estuary and Batemans Bay for 2030 and 2070, relative to the climate of 1980. Source: Hennessy et al. (2004)*

| Season | 2030 | 2070 |
|---|---|---|
| **Changes in the intensity of extreme rainfall events for the Wooli Wooli Estuary (%)** | | |
| Annual | -10 to 0 | -10 to +10 |
| Summer | -10 to +20 | -10 to +20 |
| Autumn | -20 to 0 | -10 to 0 |
| Winter | -10 to +10 | -10 to 0 |
| Spring | -10 to +10 | 0 to +20 |
| **Changes in the intensity of extreme rainfall events for Batemans Bay (%)** | | |
| Annual | -10 to +10 | -10 to 0 |
| Summer | 0 to +10 | -10 to +10 |
| Autumn | -10 to 0 | 0 to +10 |
| Winter | -10 to 0 | -10 to 0 |
| Spring | -10 to +10 | -10 to +10 |

## 6.2. Drought Frequency

Drought is a phenomenon that has meteorological, hydrological, agricultural and socio-economic perspectives. Mpelasoka et al. (2007) defined drought frequency in terms of both a purely meteorological definition, based on rainfall deficiency, and a definition better able to characterise hydrological and agricultural drought, based on soil moisture deficiency. Mpelasoka et al. (2007) used output of the CSIRO Mark2 and the Canadian Climate Center's CCCma1 climate models, selected on the basis of superior reproduction of average conditions for the current climate of Australia, to produce projections of drought frequency for Australia for 2030 and 2070.

Daily spatially interpolated rainfall and evaporation observations for the 1970-2004 period were available from the Queensland Department of Natural Resources and Mines for a set of grid points covering Australia with a resolution of 0.25°. For each grid point, monthly values of a drought index based on rainfall deficiency (RDDI) and a drought index based on soil moisture deficiency (SMDDI) were calculated from the meteorological observations. Projected changes in monthly average values of rainfall and evaporation were then applied to the observations and monthly values of the indices were then calculated for each of the climates of the years 2030 and 2070. This was done for a set of four scenarios of regional climate change (see Table 12) arising from the combination of the responses of the Australian climate to global warming in the Mark2 and CCCma1 models with global warming values for low-end and high-end global warming scenarios (see Table 1). Finally, the decadal average numbers of consecutive months per year for which the RDDI and SMDDI values indicated drought were calculated for the 1970-2004 period and the climates of the years 2030 and 2070.

***Table 12:*** *Scenarios of regional climate change considered by Mpelasoka et al. (2007).*

| Scenario | Description |
|---|---|
| **Mark2 Low GW** | Regional climate response to global warming of **Mark2** combined with a **low**-end value of the likely increase in global average temperature. |
| **Mark2 High GW** | Regional climate response to global warming of **Mark2** combined with the **high**-end value of the likely increase in global average temperature. |
| **CCCma1 Low GW** | Regional climate response to global warming of **CCCma1** combined with a **low**-end value of the likely increase in global average temperature. |
| **CCCma1 High GW** | Regional climate response to global warming of **CCCma1** combined with a **high**-end value of the likely increase in global average temperature. |

Monthly observed values of RDDI and SMDDI based on the Queensland Department of Natural Resources and Mines data indicate that for most of the Southeast Coast Drainage Division, of which the drainage basins of the Wooli Wooli and Clyde rivers are part, drought conditions were present for 10 to 20% of months during the 1974-2003 period. The results of Mpelasoka et al. (2007) for both rainfall deficiency and soil moisture deficiency for the Southeast Coast Drainage Division suggest an increase in the frequency of drought of up to 20% for all four regional climate change scenarios considered for 2030 and for both Low GW scenarios for 2070. It is suggested that increases of up to 40% are possible for parts of the Southeast Coast Drainage Division for both High GW scenarios for 2070. Applying the projections of drought frequency to the observations suggests drought in up to 24% of months per decade for all four regional climate change scenarios considered for 2030 and for both Low GW scenarios for 2070 and drought in up to 28% of months per decade for parts of the Southeast Coast Drainage Division for both High GW scenarios for 2070.

# 7. SUMMARY AND RECOMMENDATIONS

This report has drawn on existing literature to provide climate change projections for the Wooli Wooli Estuary and Batemans Bay for 2030 and 2070. Projections are given for:

- Annual and seasonal average air temperatures
- Annual and seasonal average rainfall totals
- Annual and seasonal average solar radiation
- Annual and seasonal dominant wind conditions
- Storm surge heights
- Mean sea level
- Intensity of extreme rainfall events
- Drought frequency

Most of the climate change projections given in the report by McInnes et al. (2007) that accompanies this report were based on the output of two climate model simulations, CCM2 and CCM3. In this report, where they have been available, projections derived from the same two simulations have been presented in order to describe climate change scenarios that are consistent with the information from the work of McInnes et al. (2007). These are summarised in Tables 13 and 14. Both simulations were forced with historical atmospheric greenhouse gas concentrations until 1990 and with estimates of future atmospheric greenhouse gas concentrations arising from the SRES A2 emission scenario from then on.

For some climate variables it has been possible to combine the CCM2 and CCM3 responses of the regional climate to global warming with global warming values for low-end and high-end global warming scenarios, yielding four regional climate change scenarios. The differences between the projections presented in this report for different possible regional climate change scenarios reflect the inherent uncertainty in projections of future climate conditions. Future studies of the impacts of climate change on the Wooli Wooli and Clyde River/Batemans Bay estuary systems based on the report should ideally consider all four scenarios. For some variables two scenarios have been provided that are consistent with the model responses to the mid to high estimates of future atmospheric greenhouse gas concentrations arising from the SRES A2 emission scenario. For these variables, changes given for CCM2 should be used in conjunction with the CCM2 Low GW and CCM2 High GW changes in the four-scenario variables. Similarly, changes given for CCM3 should be used in conjunction with the CCM3 Low GW and CCM3 High GW changes in the four-scenario variables. It should be noted that the four scenarios may not produce the most extreme possible estuarine impacts. It is possible that scenarios resulting in more extreme estuarine impacts than the ones given may arise from an assessment of the regional climate responses to global warming from a larger number of models and the consideration of low-end and high-end global warming scenarios for every climate variable. It is also possible that the most extreme estuarine response arises as a result of a global warming scenario that is neither low-end nor high-end. This can be investigated by obtaining changes for intermediate global warming scenarios by interpolating between the changes for the Low GW and High GW scenarios given here.

***Table 13:*** *Summary of climate change projections for the Wooli Wooli Estuary for 2030 and 2070 derived from the CCM2 and CCM3 simulations. Changes in mean sea level are relative to global average mean sea level rise, which is projected to be 0.18 to 0.79m by 2095, relative to the global average mean sea level for 1990. Other changes are relative to climatological averages for 1990. Unsigned numbers in red indicate increases. Numbers in blue indicate decreases. Source: Holper et al. (2006) and McInnes et al. (2007).*

| 2030 | | | | 2070 | | | |
|---|---|---|---|---|---|---|---|
| CCM2 Low GW | CCM2 High GW | CCM3 Low GW | CCM3 High GW | CCM2 Low GW | CCM2 High GW | CCM3 Low GW | CCM3 High GW |
| **Changes in annual average daily maximum air temperatures (℃)** | | | | | | | |
| 0.5 | 1.2 | 0.6 | 1.3 | 1.1 | 3.6 | 1.2 | 4.0 |
| **Changes in annual average daily minimum air temperatures (℃)** | | | | | | | |
| 0.5 | 1.1 | 0.6 | 1.3 | 1.1 | 3.5 | 1.2 | 4.0 |
| **Changes in annual average rainfall totals (%)** | | | | | | | |
| -3 | -6 | 0 | 0 | -6 | -19 | 0 | -1 |
| **Changes in annual average solar radiation (%)** | | | | | | | |
| 0.3 | 0.6 | 0.2 | 0.5 | 0.6 | 1.8 | 0.5 | 1.6 |
| **CCM2** | | **CCM3** | | **CCM2** | | **CCM3** | |
| **Annual dominant wind direction** | | | | | | | |
| SE (112.5 to 157.5°) | | | | | | | |
| **Changes in the frequency of annual dominant wind direction days with average wind speeds greater than 8m/s (%)** | | | | | | | |
| -4 | | 5 | | -8 | | 9 | |
| **Changes in the 1-in-100 year storm surge height (%)** | | | | | | | |
| -1 | | 1 | | -3 | | 4 | |
| **Changes in mean sea level, relative to global average mean sea level rise (m)** | | | | | | | |
| 0 to 0.04 | | 0.04 to 0.08 | | 0 to 0.04 | | 0.08 to 0.12 | |

***Table 14:*** *Summary of climate change projections for Batemans Bay for 2030 and 2070 derived from the CCM2 and CCM3 simulations. Changes in mean sea level are relative to global average mean sea level rise, which is projected to be 0.18 to 0.79m by 2095, relative to the global average mean sea level for 1990. Other changes are relative to climatological averages for 1990. Unsigned numbers in red indicate increases. Numbers in blue indicate decreases. Source: Holper et al. (2006) and McInnes et al. (2007).*

| 2030 | | | | 2070 | | | |
|---|---|---|---|---|---|---|---|
| CCM2 Low GW | CCM2 High GW | CCM3 Low GW | CCM3 High GW | CCM2 Low GW | CCM2 High GW | CCM3 Low GW | CCM3 High GW |
| **Changes in annual average daily maximum air temperatures (℃)** | | | | | | | |
| 0.5 | 1.1 | 0.7 | 1.5 | 1.1 | 3.4 | 1.4 | 4.6 |
| **Changes in annual average daily minimum air temperatures (℃)** | | | | | | | |
| 0.4 | 1.0 | 0.6 | 1.4 | 1.0 | 3.1 | 1.3 | 4.3 |
| **Changes in annual average rainfall totals (%)** | | | | | | | |
| -3 | -8 | 4 | 10 | -7 | -23 | 9 | 30 |
| **Changes in annual average solar radiation (%)** | | | | | | | |
| 0.1 | 0.2 | 0.1 | 0.3 | 0.2 | 0.6 | 0.3 | 0.8 |
| **CCM2** | | **CCM3** | | **CCM2** | | **CCM3** | |
| **Annual dominant wind direction** | | | | | | | |
| SW (202.5 to 247.5°) | | | | | | | |
| **Changes in the frequency of annual dominant wind direction days with average wind speeds greater than 8m/s (%)** | | | | | | | |
| -1 | | 2 | | -2 | | 8 | |
| **Changes in the 1-in-100 year storm surge height (%)** | | | | | | | |
| -1 | | 1 | | -3 | | 1 | |
| **Changes in mean sea level, relative to global average mean sea level rise (m)** | | | | | | | |
| 0 to 0.04 | | 0 to 0.04 | | 0 to 0.04 | | 0.08 to 0.12 | |

In addition to the climate change projections presented in Tables 13 and 14, projections that include information from climate simulations other than CCM2 and CCM3 are available for rainfall extremes. These are summarised in Table 15.

***Table 15:*** *Summary of climate change projections for rainfall extremes for the Wooli Wooli Estuary and Batemans Bay for 2030 and 2070. Changes in the intensity of extreme rainfall events are relative to the climate of 1980. Source: Hennessy et al. (2004) and Mpelasoka et al. (2007).*

| Location | 2030 | 2070 |
|---|---|---|
| **Changes in the intensity of extreme rainfall events analysed on an annual basis (%)** | | |
| Wooli Wooli Estuary | -10 to 0 | -10 to +10 |
| Batemans Bay | -10 to +10 | -10 to 0 |
| **Drought frequency (% of months per decade)** | | |
| Southeast Coast Drainage Division | < 24 | < 28 |

## ACKNOWLEDGMENTS

The work of the authors draws upon research findings of many colleagues within CSIRO Marine and Atmospheric Research and overseas research institutions. CSIRO climate models were developed by the members of the Climate, Weather and Ocean Prediction Theme of CSIRO Marine and Atmospheric Research.

The authors wish to acknowledge valuable comments on drafts of this report made by Rosh Ranasinghe of the New South Wales Department of Environment and Climate Change and Dewi Kirono of CSIRO Marine and Atmospheric Research. Valuable discussions on the content of the report were held with Deborah Abbs, Kevin Hennessy and Janice Bathols of CSIRO Marine and Atmospheric Research and Freddie Mpelasoka of CSIRO Land and Water.

## REFERENCES


Gordon, H. B., L. D. Rotstayn, J. L. McGregor, M. R. Dix, E. A. Kowalczyk, L. J. Waterman, A. C> Hirst, S. G. Wilson, M. A. Collier, I. G. Watterson and T. I. Elliott, 2002: The CSIRO Mk3 climate system model. CSIRO Atmospheric Research Technical Paper No. 60, 134pp.

Hennessy, K. J., K. L. McInnes, D. J. Abbs, R. N. Jones, J. M. Bathols, R. Suppiah, J. R. Ricketts, A. S. Rafter, D. Collins and D. Jones, 2004: Climate change in New South Wales. Part 2: Projected changes in climate extremes. A report for the New South Wales Greenhouse Office by CSIRO Marine and Atmospheric Research and the Australian Bureau of Meteorology, 79 pp.

Hirst, A. C., S. P. O'Farrell, and H. B. Gordon, 2000: Comparison of a coupled ocean-atmosphere model with and without oceanic eddy-induced advection. Part I: Ocean spinup and control integrations. Journal of Climate, 13 (1), 139-163.

Holper, P. N., S. Lucy, M. Nolan, C. Senese and K. J. Hennessy, 2006: Infrastructure and Climate Change Risk Assessment for Victoria. A consultancy report for the Victorian Government by CSIRO Marine and Atmospheric Research, Maunsell Australia and Phillips Fox, 84 pp.

IPCC, 2000: Special Report on Emission Scenarios: A Special Report of Working Group III of the Intergovernmental Panel on Climate Change. Cambridge University Press.

IPCC, 2001: Climate Change 2001: The Scientific Basis. Contribution of Working Group I to the Third Assessment Report of the Intergovernmental Panel on Climate Change. Cambridge University Press.

IPCC, 2007: Climate Change 2007: The Physical Science Basis. Contribution of Working Group I to the Fourth Assessment Report of the Intergovernmental Panel on Climate Change. Summary for Policymakers. Cambridge University Press.

Kalnay, E., M. Kanamitsu, R. Kistler, W. Collins, D. Deaven, L. Gandin, M. Iredell, S. Saha, G. White, J. Woollen, Y. Zhu, A. Leetmaa, B. Reynolds, M. Chelliah, W. Ebisuzaki, W. Higgins, J. Janowiak, K. C. Mo, C. Ropelewski, J. Wang, R. Jenne and D. Joseph, 1996: The NCEP/NCAR 40-Year Reanalysis Project. Bulletin of the American Meteorological Society, 77, 437–471.

McGregor, J. L., 2005: C-CAM: Geometric aspects and dynamical formulation. CSIRO Atmospheric Research Technical Paper No. 70, 43 pp.

McGregor, J. L., and M. R. Dix, 2001: The CSIRO conformal-cubic atmospheric GCM. In IUTAM Symposium on Advances in Mathematical Modelling of Atmosphere and Ocean Dynamics, P. F. Hodnett (Ed.), Kluwer, Dordrecht, 197-202.

McInnes, K. L., D. J. Abbs, S. P. O'Farrell, I. Macadam, J. G. O'Grady and R. Ranasinghe, 2007: Projected changes in climatological forcing for coastal erosion in NSW. A report for the New South Wales Department of Environment and Climate Change by CSIRO Marine and Atmospheric Research.

Mpelasoka, F., K. J. Hennessy, R. N. Jones and B. Bates, 2007: Comparison of suitable drought indices for climate change impacts assessment over Australia towards resource management. International Journal of Climatology (accepted).

Whetton, P. H., K. L. McInnes, R. N. Jones, K. J. Hennessy, R. Suppiah, C. M. Page, J. M. Bathols and P. Durack, 2005: Australian climate change projections for impact assessment and policy application: A review. CSIRO Marine and Atmospheric Research Paper No. 1, 33 pp.

**Contact Us**
Phone: 1300 363 400
+61 3 9545 2176
Email: enquiries@csiro.au
Web: www.csiro.au

## Your CSIRO

Australia is founding its future on science and innovation. Its national science agency, CSIRO, is a powerhouse of ideas, technologies and skills for building prosperity, growth, health and sustainability. It serves governments, industries, business and communities across the nation.